Vehicle Braking Strategies Based on Regenerative Braking Boundaries of Electric Machines

Aravind Samba Murthy, David P. Magee and David G. Taylor

***Abstract*—Electric and hybrid-electric vehicles are capable of providing electrical braking to assist mechanical brakes during a braking event. Braking strategies can be formulated to dictate the manner in which the braking effort is shared between the electrical and mechanical brakes. Electrical braking capability is identified by regions in the braking quadrants of an electric machine's torque-speed plane, and these capability regions may be further subdivided into regenerative and non-regenerative braking regions. Regenerative electrical braking adds energy to the energy storage system, whereas non-regenerative electrical braking subtracts energy from the energy storage system. This paper uses the concept of regenerative braking boundaries to define braking strategies that avoid operation in non-regenerative braking regions so as to recover as much electrical energy as possible during braking events.**

I. Introduction

Electric and hybrid-electric vehicles incorporate a combination of electrical and mechanical braking systems. The electrical braking system has two modes of operation, referred to as regenerative braking and non-regenerative braking; during an electrical braking event, the former adds energy to the energy storage system whereas the latter subtracts energy from the energy storage system. With regenerative braking, the kinetic energy of the vehicle is recovered, so an electric vehicle travels further before depleting its battery and a hybrid-electric vehicle consumes less fuel to travel a particular distance.

The overall braking torque is requested by the driver, so a braking strategy is required to determine how braking effort is shared between the electrical and mechanical braking systems. Design of a braking strategy involves consideration of vehicle stability [1] and kinetic energy recovery. Some studies recommend maximal use of electrical braking above a threshold speed, along with pure mechanical braking below the threshold speed [2], [3]. Other studies recommend smoothly varying the level of electrical braking throughout a braking event, from maximum level to zero level [4], [5]. However, none of these studies provides a physical basis for the choice of braking strategy design coefficients such as threshold speed or ramp-down rate.

In this paper, vehicle braking strategies are designed using the concept of steady-state electric machine regenerative braking boundaries. A framework for determining regenerative braking boundaries was reported in [6] for converter-controlled permanent-magnet synchronous machines, but that work did not consider the application of the concept to vehicle braking strategies. Regenerative braking boundaries are curves in the torque-speed plane that demarcate the regenerative braking region from the non-regenerative braking region. Equipped with knowledge of the regenerative braking boundaries, it becomes possible to formulate braking strategies that adhere to the driver's braking torque request while attempting to recover as much kinetic energy as possible. This paper formulates several different braking strategies and studies their impact on the energy consumption of an electric vehicle using typical drive schedules.

This work was supported in part by Texas Instruments.

Aravind Samba Murthy is with Georgia Institute of Technology, School of Electrical and Computer Engineering, Atlanta, GA 30332 USA.

David P. Magee is with Texas Instruments, Embedded Processor Systems Lab, Dallas, TX 75243 USA.

David G. Taylor is with Georgia Institute of Technology, School of Electrical and Computer Engineering, Atlanta, GA 30332 USA.

II. Electric Machine System

A. Modeling

A schematic diagram of the electric machine system is shown in Fig. 1. The focus here is on interior permanent-magnet (IPM) synchronous machines which are modeled under steady-state assumptions in the dq reference frame so as to account for both copper and iron losses; the two types of losses are associated with two current flow paths, i.e. the magnetizing currents are not the same as the terminal currents.

The electromagnetic torque is modeled by

$$T = N\left(\Lambda + (L_d - L_q) i_{dm}\right) i_{qm} \tag{1}$$

where N is the number of permanent-magnet pole pairs, Λ is the rotor flux coefficient, L_d and L_q are the stator inductance coefficients, and i_{dm} and i_{qm} are the magnetizing components of the stator currents. The voltage equations are

$$\begin{aligned} -v_d + Ri_d + R_i(i_d - i_{dm}) &= 0 \\ -v_q + Ri_q + R_i(i_q - i_{qm}) &= 0 \\ R_i(i_{dm} - i_d) - N\omega\left(L_q i_{qm}\right) &= 0 \\ R_i(i_{qm} - i_q) + N\omega\left(L_d i_{dm} + \Lambda\right) &= 0 \end{aligned} \tag{2}$$

where R is the copper-loss resistance, R_i is the iron-loss resistance, i_d and i_q are the terminal components of the stator currents, v_d and v_q are the applied stator voltages, and ω is the rotor speed. The applied stator voltages are determined by control according to

$$v_d = u_d\, v_{\rm bus}, \quad v_q = u_q\, v_{\rm bus} \tag{3}$$

where u_d and u_q are duty cycle commands and $v_{\rm bus}$ is the dc bus voltage. Assuming a lossless power converter, the dc bus current satisfies

$$i_{\rm bus} = u_d i_d + u_q i_q. \tag{4}$$

978-1-4673-6741-7/15/$31.00 ©2015 IEEE

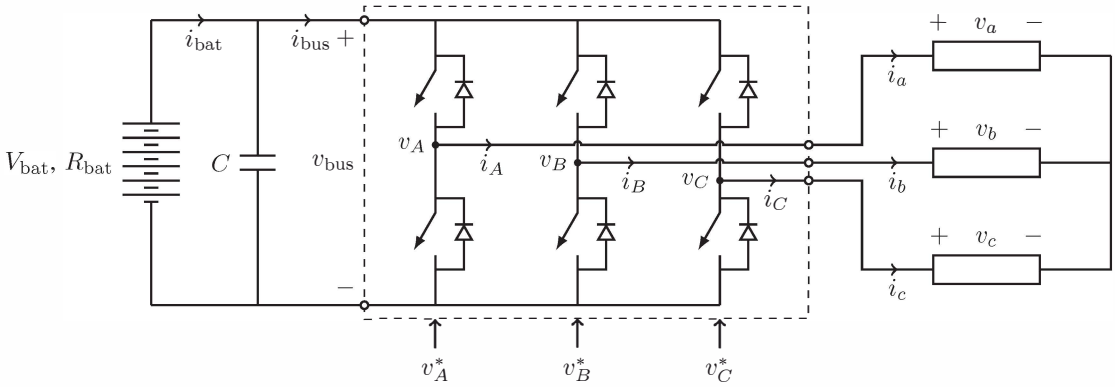

Fig. 1: Schematic diagram of the wye-connected electric machine system.

Since $i_{\rm bat} = i_{\rm bus}$, the dc bus voltage satisfies

$$v_{\rm bus} = V_{\rm bat} - R_{\rm bat} i_{\rm bus}. \tag{5}$$

The electrical losses consist of three components:

$$\begin{aligned} W_{\rm copper} &= R\left(i_d^2 + i_q^2\right) \\ W_{\rm iron} &= R_i\left(\left(i_d - i_{dm}\right)^2 + \left(i_q - i_{qm}\right)^2\right) \\ W_{\rm battery} &= R_{\rm bat} i_{\rm bus}^2 \end{aligned} \tag{6}$$

The duty cycle commands and the terminal currents must satisfy the operational constraints

$$\begin{aligned} \|u_{dq}\| &= \sqrt{u_d^2 + u_q^2} \le U_{\max} \\ \|i_{dq}\| &= \sqrt{i_d^2 + i_q^2} \le I_{\max} \end{aligned} \tag{7}$$

where $U_{\max}$ and $I_{\max}$ are fixed parameters. Table I lists the parameter values for the electric machine system considered in this section and used in the electric vehicle examples of the following sections.

B. Optimization

The torque-speed capability of the electric machine system for forward rotation, and in particular its braking capability region and its regenerative braking capability region, are determined by solving the following optimization problems.

P1) For any feasible value of $\omega \ge 0$:

$$\begin{aligned} \text{maximize} \quad & T \\ \text{subject to} \quad & \text{(1)–(5)}, \ T \ge 0 \\ & \|u_{dq}\| \le U_{\max}, \ \|i_{dq}\| \le I_{\max}. \end{aligned}$$

P2) For any feasible value of $\omega \ge 0$:

$$\begin{aligned} \text{minimize} \quad & T \\ \text{subject to} \quad & \text{(1)–(5)}, \ T \le 0 \\ & \|u_{dq}\| \le U_{\max}, \ \|i_{dq}\| \le I_{\max}. \end{aligned}$$

P3) For any feasible value of $\omega \ge 0$:

$$\begin{aligned} \text{maximize} \quad & T \\ \text{subject to} \quad & \text{(1)–(5)}, \ T \le 0 \\ & \|u_{dq}\| \le U_{\max}, \ \|i_{dq}\| \le I_{\max}. \end{aligned}$$

TABLE I: Electric Vehicle Parameters

Parameter	Symbol	Value	Units
vehicle mass	m_v	1653.8	kg
mass factor	δ_m	1.04	—
wheel radius	r_w	0.316	m
frontal area	a_f	2.7435	$\rm m^2$
drag coefficient	c_d	0.26	—
rolling resistance coefficient	c_r	0.0069	—
gear ratio	ξ	8.125	—
gear efficiency	η	95	%
pole pairs	N	4	—
copper loss resistance	R	0.297	Ω
iron loss resistance	R_i	240	Ω
d-axis inductance	L_d	0.5841	mH
q-axis inductance	L_q	0.6039	mH
rotor flux	Λ	0.235	Wb
current vector limit	$I_{\max}$	300	A
duty cycle vector limit	$U_{\max}$	0.707	—
open-circuit voltage	$V_{\rm bat}$	366.3	V
internal resistance	$R_{\rm bat}$	24.7	mΩ
energy capacity		24.72	kWh
charge capacity		67.5	Ah
initial state of charge		90	%

P4) For any feasible value of $\omega \ge 0$:

$$\begin{aligned} \text{minimize} \quad & T \\ \text{subject to} \quad & \text{(1)–(5)}, \ T \le 0, \ i_{\rm bus} \le 0 \\ & \|u_{dq}\| \le U_{\max}, \ \|i_{dq}\| \le I_{\max}. \end{aligned}$$

P5) For any feasible value of $\omega \ge 0$:

$$\begin{aligned} \text{maximize} \quad & T \\ \text{subject to} \quad & \text{(1)–(5)}, \ T \le 0, \ i_{\rm bus} \le 0 \\ & \|u_{dq}\| \le U_{\max}, \ \|i_{dq}\| \le I_{\max}. \end{aligned}$$

P6) For any feasible value of $\omega \ge 0$:

$$\begin{aligned} \text{minimize} \quad & i_{\rm bus} \\ \text{subject to} \quad & \text{(1)–(5)}, \ T \le 0 \\ & \|u_{dq}\| \le U_{\max}, \ \|i_{dq}\| \le I_{\max}. \end{aligned}$$

P1 determines motoring torque limits, P2 and P3 determine upper and lower braking torque limits, and P4 and P5 determine upper and lower regenerative braking torque limits. P6

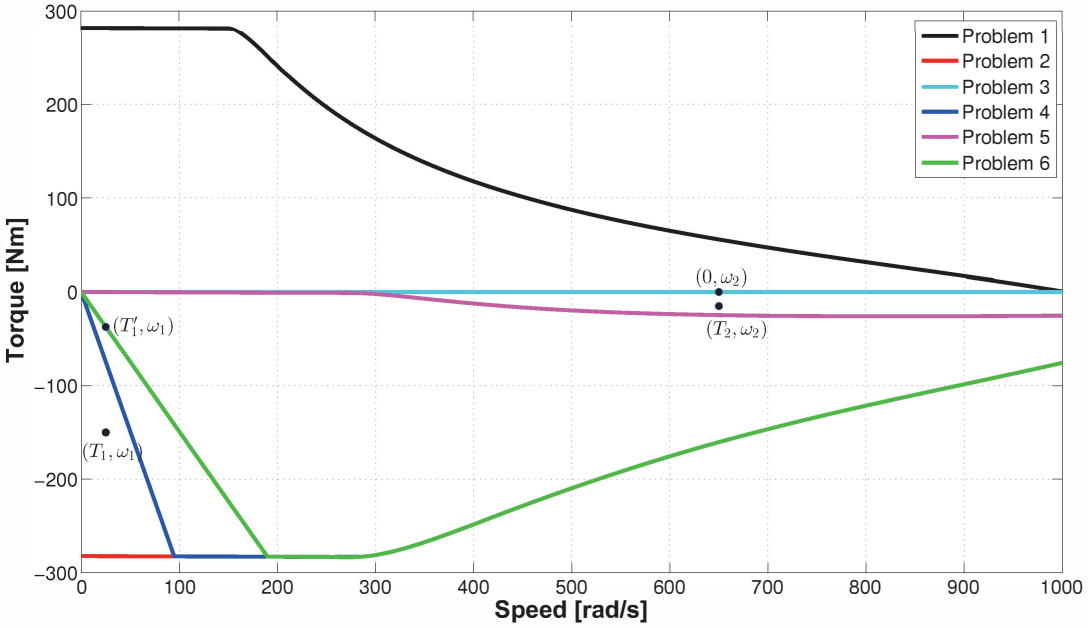

Fig. 2: Operating region boundaries and representative operating points.

determines the conditions that maximize the dc bus current flowing into the energy storage system when performing regenerative braking. The numerically computed solutions to these optimization problems are shown in Fig. 2. From this figure, it can be seen that there are two separate regions associated with non-regenerative braking; the low-speed region between the torque axis and the solution to P4, and the high-speed region between the speed axis and the solution to P5.

If speed is dictated, as in vehicular applications, then it remains to consider how torque will be developed at operating points within the torque-speed capability region, identified by solutions of P1 and P2. Since torque is a scalar quantity but the control input is a vector quantity, a specified torque may be produced in more than one way. The approach taken here is to minimize the electrical losses modeled in (6), by solving the following optimization problem (see [7]).

P7) For any feasible values of T and $\omega \geq 0$:

$$\begin{array}{ll} \text{minimize} & W_{\text{copper}} + W_{\text{iron}} + W_{\text{battery}} \\ \text{subject to} & (1)\text{–}(6) \\ & \|u_{dq}\| \leq U_{\max},\ \|i_{dq}\| \leq I_{\max}. \end{array}$$

Given a minimum-loss solution at a specified torque-speed operating point, it is of interest to determine the corresponding power conversion efficiency. For this purpose, electrical power and mechanical power are defined by

$$P_e = V_{\text{bat}} i_{\text{bus}}, \quad P_m = T\omega \tag{8}$$

where mechanical spin loss has been neglected. The power conversion efficiency is defined as

$$\eta = \begin{cases} P_m/P_e & , \text{ if } P_m > 0 \text{ and } P_e > 0 \\ P_e/P_m & , \text{ if } P_m < 0 \text{ and } P_e < 0 \\ 0 & , \text{ otherwise} \end{cases} \tag{9}$$

where non-regenerative braking, which does not result in conversion of power, is assigned an efficiency of zero. The solution of P7 is displayed in Fig. 3(a), in terms of losses, and in Fig. 3(b), in terms of efficiency.

III. Vehicle Braking System

A. Modeling

Though a braking event is a transient phenomenon for a vehicle, the electric machine producing braking torque experiences quasi-steady-state operation (i.e. its torque-speed operating point varies slowly relative to the electrical time scale, due to large vehicle inertia). For this reason, the regenerative braking boundaries, which have been defined using steady-state assumptions, can be expected to provide information that is relevant to the study of kinetic energy recovery and thus useful for design of vehicle braking strategies.

In this and the following section, a numerical example is considered in detail. The example involves an electric vehicle, driven through a fixed gear by an IPM synchronous machine fed by a power converter that is connected to a battery pack, as described in the previous section. The electric power flow is determined from a lookup table populated with system loss values on a discrete grid of torque and speed points; the lookup

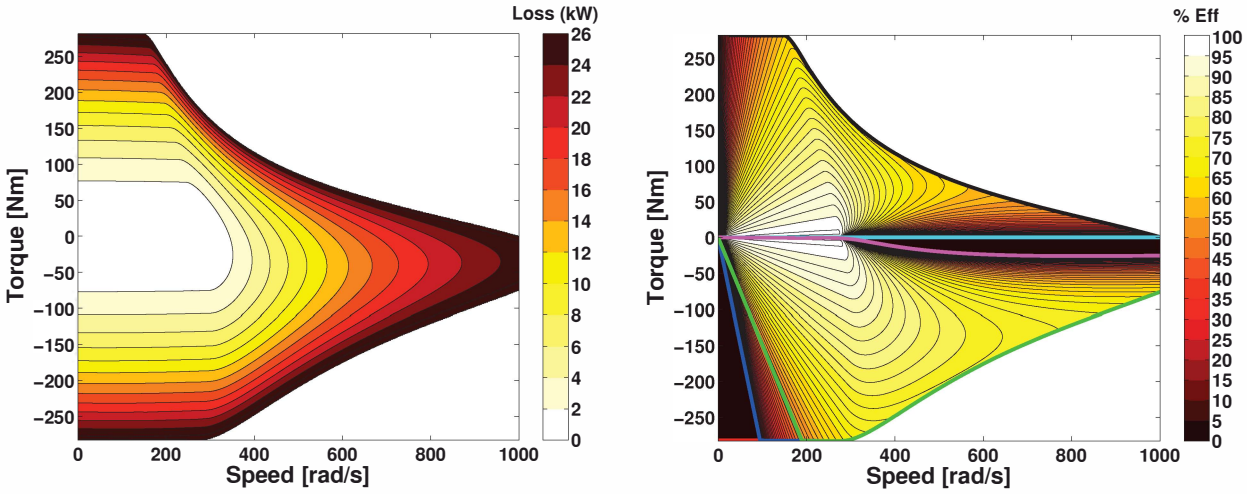

(a) Loss map

(b) Efficiency map

Fig. 3: Loss and efficiency maps for operating points in torque-speed capability region.

table is computed off-line and is based on loss-minimization. The given vehicle parameters are displayed in Table I.

Assuming forward driving with no wind and no incline, the force F required for a vehicle to follow a drive schedule specifying vehicle speed v at time t is given by

$$F = c_r m_v g + \tfrac{1}{2}\rho_a a_f c_d v^2 + \delta_m m_v \frac{dv}{dt} \tag{10}$$

where m_v is vehicle mass, δ_m is mass factor, a_f is frontal area, c_d is aerodynamic drag coefficient and c_r is rolling resistance coefficient; non-specific parameters are mass density of air ρ_a and acceleration of gravity g. The corresponding electric machine torque-speed operating point is determined by

$$T = \left(\frac{r_w}{\xi_g \eta_g}\right) F, \quad \omega = \left(\frac{\xi_g}{r_w}\right) v \tag{11}$$

where r_w is wheel radius, ξ_g is gear ratio and η_g is gear efficiency. Given a drive schedule, (10) and (11) provide the time trajectory of corresponding torque-speed operating points.

B. Strategies

The design of vehicle braking strategies begins with the formulation and solution of a set of optimization problems (P1 through P6), resulting in a set of curves in the torque-speed plane. The discussion below refers to the set of curves and representative operating points displayed in Fig. 2.

Operating point (T_1, ω_1) is located in the low-speed non-regenerative braking region. Accepting such an operating point results in removal of energy from the energy storage system. In this case, it would be wise to replace the given operating point by (T_1', ω_1), since this would result in maximum regenerative current. With this modification, the required mechanical braking torque would be

$$T_{\text{mech}} = (T_1 - T_1')\,\xi_g \eta_g. \tag{12}$$

TABLE II: Vehicle Braking Strategies

Strategy I	Braking mode: mechanical (all operating points shifted) Low-speed non-regenerative operating points: n/a High-speed non-regenerative operating points: n/a
Strategy II	Braking mode: electrical and mechanical Low-speed non-regenerative operating points: do not shift High-speed non-regenerative operating points: do not shift
Strategy III	Braking mode: electrical and mechanical Low-speed non-regenerative operating points: shift High-speed non-regenerative operating points: shift
Strategy IV	Braking mode: electrical and mechanical Low-speed non-regenerative operating points: shift High-speed non-regenerative operating points: do not shift

This strategy applies to all operating points located below the maximum regenerative current curve; this includes all points in the non-regenerative braking region, as well as some points in the regenerative braking region.

Operating point (T_2, ω_2) is located in the high-speed non-regenerative braking region. Accepting such an operating point results in removal of energy from the energy storage system, so it is natural to seek some alternative. One may be tempted to think that the power drain would be reduced if the given operating point is replaced by $(0, \omega_2)$, since this would reduce the electric braking torque to zero. If such a modification is made, the required mechanical braking torque would be

$$T_{\text{mech}} = T_2 \xi_g \eta_g. \tag{13}$$

In this case, the modified operating point would be further away from the zero electric power boundary (i.e. the regenerative braking boundary), thus resulting in larger power drain.

Motivated by the discussion above, four vehicle braking strategies have been defined for further study; see Table II. Strategy I uses only mechanical braking, whereas Strategy II adds electrical braking. Strategy III and Strategy IV consider various operating point modifications; modification of

low-speed non-regenerative operating points is expected to improve power flow into the energy storage system, whereas modification of high-speed non-regenerative operating points is expected to degrade the power flow from the energy storage system. Note that operating point modifications change torque values, but not speed values; the speed values cannot be modified, since the electric machine speed is dictated by the drive-schedule-required vehicle speed and the fixed gear ratio.

IV. Simulation Results

The four braking strategies were investigated by running detailed simulations with the following drive schedules:

- UDDS, Urban Dynamometer Driving Schedule;
- FTP, Federal Test Procedure;
- US06, Supplemental Federal Test Procedure;
- NYCC, New York City Cycle.

At each time instant, the required speed is obtained from the drive schedule, the required force is computed from (10), and the required electric machine operating point is computed from (11). Fig. 4 shows the electric machine operating points associated with each braking strategy, as defined in Table II; also shown for reference are the motoring torque boundary (P1), the braking torque boundaries (P2 and P3), the regenerative braking torque boundaries (P4 and P5) and the torque-speed curve associated with maximum regenerative current (P6).

- Fig. 4 (a) represents Strategy I
  - All operating points originally located anywhere in the braking region have been shifted so that the requested torque is zero.
- Fig. 4 (b) represents Strategy II
  - All operating points originally located anywhere in the braking region have been used as is without modification.
- Fig. 4 (c) represents Strategy III
  - All operating points originally located in the regenerative braking region have been used as is without modification.
  - All operating points originally located in the low-speed non-regenerative braking region have been shifted so that the requested torque lies on the maximum regenerative current line.
  - All operating points originally located in the high-speed non-regenerative braking region have been shifted so that the requested torque is zero.
- Fig. 4 (d) represents Strategy IV
  - All operating points originally located in the regenerative braking region have been used as is without modification.
  - All operating points originally located in the low-speed non-regenerative braking region have been shifted so that the requested torque lies on the maximum regenerative current line.
  - All operating points originally located in the high-speed non-regenerative braking region have been used as is without modification.

TABLE III: Simulation Results

Schedule	Energy Consumption (Wh/mile)			
	Strategy I	Strategy II	Strategy III	Strategy IV
UDDS	320.83	227.29	231.86	226.92
FTP	352.93	260.73	266.71	260.39
US06	689.89	593.67	602.57	593.32
NYCC	328.40	158.39	157.50	157.44

Differences between the braking strategies are visually evident from the variations in electric machine operating point locations within the braking quadrant. In this example, pure electrical braking is always feasible, so mechanical braking is used only as needed to decrease electrical energy usage; more generally, mechanical braking would also be needed if a braking request exceeds electrical braking capability.

It is important to understand that, for each braking strategy, every vehicle operating point generates a corresponding electric machine operating point, and all of these electric machine operating points appear in Fig. 4. The electric machine is not clutched, so its rotor must always rotate at a speed dictated by the vehicle speed, even during a braking event. As shown in the previous section, when iron losses are accounted for, operation of an electric machine at non-zero speed will consume some level of electric power even if its requested torque is zero.

Each electric machine operating point identified in Fig. 4 will be associated with either battery discharging or battery charging, as indicated in Fig. 3. Points of Fig. 4 in the 1st quadrant, as well as the non-regenerative regions of the 4th quadrant, all correspond to battery discharging, whereas points of Fig. 4 in the regenerative region of the 4th quadrant all correspond to battery charging, as seen from Fig. 3. The penalty or reward associated with operation at a particular operating point is determined from the solution to P7, as displayed in Fig. 3, using (6), (8) and (9).

Energy consumption results are shown in Table III, and in every case they agree with the intuition developed from prior analysis of the regenerative braking boundaries. Strategy II outperforms Strategy I by allowing for use of electrical braking in a non-discriminant manner; this makes sense because most electrical braking operating points generated by the drive schedules are located within the regenerative braking region. Strategy III should be expected to outperform Strategy II on drive schedules that generate more low-speed than high-speed non-regenerative operating points; this intuition is verified by the result obtained for the NYCC drive schedule. Strategy II should be expected to outperform Strategy III on drive schedules that generate more high-speed than low-speed non-regenerative operating points; this intuition is verified by the results obtained for the UDDS, FTP and US06 drive schedules. Strategy IV should be most favorable, based on appropriate handling of both low-speed and high-speed non-regenerative operating points; the results obtained agree with this intuition, as this strategy reduced energy consumption by 0.3-1.1 Wh/mile compared to Strategy II (i.e. a 100 mile

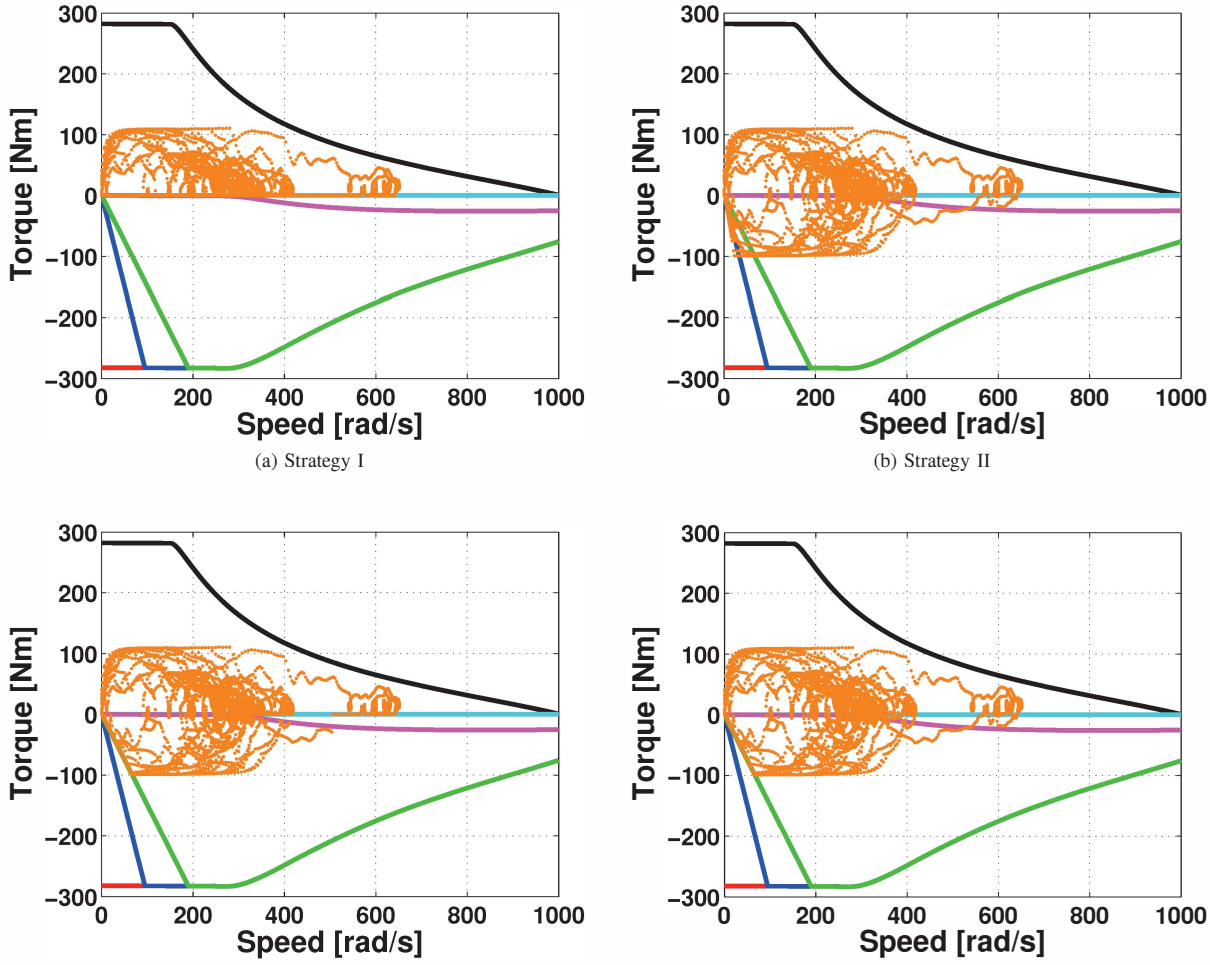

(a) Strategy I

(b) Strategy II

(c) Strategy III

(d) Strategy IV

Fig. 4: Comparison of vehicle braking strategies for the UDDS drive schedule.

excursion saves 0.03-0.11 kWh of energy).

V. Conclusion

When electric machines are used in vehicular applications, it is important to consider the boundaries of their regenerative braking capability. With knowledge of these boundaries, it is possible to develop braking strategies that avoid the electric machine's non-regenerative braking modes, thereby improving vehicle operating efficiency. An electric vehicle example has been used to illustrate the connection between regenerative braking boundaries and vehicle braking strategy design; for this example, the best vehicle braking strategy was one that avoided low-speed non-regenerative braking modes but permitted high-speed non-regenerative braking modes. More complex hybrid-electric vehicles, which involve an internal combustion engine and one or more electric machines, may require a more elaborate vehicle braking strategy, but the concept of regenerative braking boundaries is expected to play an equally important role in the development of braking strategies to improve hybrid-electric vehicle operating efficiency.

References

[1] S. Cikanek and K. Bailey, "Regenerative braking system for a hybrid electric vehicle," *American Control Conference*, pp. 3129–3134, May 2002.

[2] X. Nian, F. Peng and H. Zhang, "Regenerative braking system of electric vehicle driven by brushless DC motor," *IEEE Transactions on Industrial Electronics*, 61(10), pp. 5798–5808, Oct 2014.

[3] M. Paredes, J. Pomilio and A. Santos, "Combined regenerative and mechanical braking in electric vehicle," *Proceedings of Brazilian Power Electronics Conference*, pp. 935–941, Oct 2013.

[4] D. Crombez and J. Czubay, "Vehicle and method for controlling regenerative braking," US Patent 8,066,339 B2, Nov 2011.

[5] M. Zhou, Z. Gao and H. Zhang, "Research on regenerative braking control strategy of hybrid electric vehicle," *International Forum on Strategic Technology*, pp. 300–303, Aug 2011.

[6] A. Samba Murthy and D. Taylor, "Regenerative braking of battery powered converter controlled PM synchronous machines," *IEEE Transportation Electrification Conference and Expo*, pp. 1–6, Jun 2013.

[7] S. Morimoto, Y. Tong, Y. Takeda and T. Hirasa, "Loss minimization control of permanent magnet synchronous motor drives," *IEEE Transactions on Industrial Electronics*, 41(5), pp. 511–517, Oct 1994.